**Technical Paper**

ISSN 1997-1400 Int. J. Pavement Res. Technol. 3(3):135-141


# A Finite Element Model for Tire/Pavement Interaction: Application to Predicting Pavement Damage

Kaiming Xia

**Abstract:** Tire/pavement interaction has been an important research topic in pavement engineering for many years. Rutting and fatigue cracking are two important concerns that govern the pavement structure design. The allowable number of load repetitions to limit rutting and fatigue cracking are predicted based on the tensile stress or strain at the bottom of asphalt concrete layer and compressive strain at the top of subgrade. Traditionally, strains are calculated using multilayer elastic formulation based on the predefined contact area either circular or rectangular, which are not very accurate. A fully dynamic tire/pavement interaction satisfying impenetrability and traction conditions cannot be achieved with empirical approaches. Therefore solutions of stresses and strains at concerned places of pavement structure are not reliable. This paper presents a fully tire/pavement interaction finite element model that can effectively include the dynamic effect of tire rolling to the calculation of pavement response. The tire is modeled as a finite strain hyperelastic material, and the pavement structure is modeled as elastic materials. A finite strain hyperelasticity is introduced for modeling of rubber tire, which was implemented as a user subroutine in ABAQUS. Representative simulations are provided to demonstrate how the tire/pavement interaction model can be used to predict pavement response and pavement damage due to fatigue cracking and rutting in the field of pavement engineering.

***Key words***: *Finite element; Hyperelasticity; Pavement damage; Pavement response; Tire/pavement interaction.*

## Introduction

Asphalt pavement exhibits various distresses that will eventually lead to the pavement's failure. Dynamic vehicle loads, transferred to the pavement structure through the tire, have been considered the major factor to cause pavement distresses: rutting and fatigue cracking. Both fatigue cracking and rutting represents the two most common distresses with pavement deterioration, which are closely related to tire/pavement interaction. The vehicle load causes the pavement structure to deform, which creates both compressive and tensile stresses and strains in the asphalt pavement portion of the pavement structure. Rutting is sometimes called channeling, which represents a serious longitudinal surface depression in the vehicle wheel paths. The cumulative permanent deformations of subgrade soil and asphalt mixture are the major part of the total rutting depth. Vehicle tire compaction of unstable asphalt mixture is the dominant reason that causes rutting of asphalt concrete. Fatigue cracking is caused by repeated traffic load. The principal criterion for the fatigue of an asphalt pavement is the maximum tensile strain at the bottom of the asphalt layer, while the principal criterion for permanent deformation due to subgrade deformation is the maximum compressive strain at the top of the subgrade [1]. Cracking of asphalt pavement layer occurs from repeated tensile strains of which the maximum occurs at the bottom of the asphalt layer. The crack, once initiated, propagates upward causing gradual weakening of the asphalt pavement. Asphalt pavement usually starts to crack once the temperature or traffic generated stresses and strains exceed the fatigue or tensile strength of the compacted asphalt mixture. Once the tensile strength of the asphalt mixture is exceeded, a crack will be developed at the interface. Then the crack propagates toward the pavement surface under the repetitive traffic tire load.

Accurately estimating the response of the pavement to traffic load is very critical to predict the distress development. The tire inflation pressure and the tire structure are the two most important factors that influence the contact area and contact pressure distribution at the tire pavement interface. In the past, researchers have tried to discover which of these factors have the greatest influence on pavement response. Theoretical analyses employing various prediction models are often used in attempts to identify the critical factor or combination of factors. Prediction of pavement performance under traffic load has been developed based on the pavement mechanical performance monitored in field tests [2-8] and empirical methods [9, 10]. For pavement design, the induced horizontal tensile strains at the bottom of the asphalt layer and the vertical compressive strains at the interface with the top of the subgrade [1] are used to estimate the allowable number of load repetitions. In order to calculate these strains, the multilayer elastic theory was used [1] in which the contact pressure distribution was always assumed. The current design method for asphalt pavement adopts a relatively simple assumption to calculate the contact pressure between tire and pavement surface [6]. The contact area for general pavement design is assumed to be circular or rectangular, which is inaccurate to predict the maximum stress and strain in the pavement that usually triggers pavement damage [1]. Also the analytical formulations used to calculate these stresses and strains always assume that vertical pressures due to vehicle loads are uniform and quasi-static. The manner in which traffic loads are transferred to the pavement surface and the entire pavement structure is controlled by the tire-pavement interaction mechanism. Generally, the responses of pavement structure to traffic loads are affected by pavement stiffness, thickness, vehicle load magnitude, axle type and configuration, tire type, and pressure.

[1] Assistant Research Professor, Division of Engineering, Colorado School of Mines, Golden, CO 80401 USA.
[+] Corresponding Author: E-mail kxia@mines.edu
Note: Submitted November 19, 2009; Revised February 9, 2010; Accepted February 20, 2010.

However, this cannot be captured using the available empirical formulations. Accurately estimating the stress and strain induced by repeated vehicle load, dynamic tire/pavement interaction should be fully understood. Finite element method (FEM) is well suited to simulate tire/pavement interaction. Although FEM has been used to investigate the pavement response to external traffic load [9-13], fully dynamic tire/pavement interactions were rarely conducted in the past. Among the empirical methods, an equivalent rectangular contact area was always predefined, which is used to determine the contact pressure. The moving traffic load is applied to the elements of asphalt pavement where there is contact with tire. Therefore the real tire/pavement interaction cannot be exactly captured in these simulations. Only very few tire/pavement interaction models were carried out in the past, such as in literature [14]. Also tire/pavement interaction involves the modeling of tire-pavement frictional interface, finite strain hyperelasticity of rubber material, tire structure, multiplayer modeling of pavement system. Fully understanding this issue has a positive impact on pavement management, which can significantly reduce the need for field monitoring of pavement performance and improve the pavement design.

The goal of this paper is to present a fully dynamic FEM tire/pavement interaction model and investigate the effects of tire pressure, tire type, and axle load on the response of asphalt pavements.

## Basic Equations of Finite Deformation

For modeling of rubber material, the large deformation theory should be used. It is necessary to recognize that the deformation of material could be relatively large during a loading-unloading cycle, which in turn necessitates the clear distinguishing between the undeformed configuration and deformed configuration. For a typical time step, the updated configuration of the body at step $t_n+\Delta t$ may be written as a function of the configuration at step $t_n$ and the incremental displacement $\Delta u$ during the time step $\Delta t$. An updated position vector can be given by:

$$x_{n=1} = x + u = x_n + \Delta u \tag{1}$$

where, **u** is the total displacement vector with respect to the original configuration. The deformation gradient or intermediate deformation gradient is defined as follows:

$$\mathbf{F} = \frac{\partial \varphi}{\partial \mathbf{X}} = \mathbf{1} + \frac{\partial \mathbf{u}}{\partial \mathbf{X}} \qquad \text{or} \qquad \mathbf{f} = \frac{\partial \mathbf{x}_{n+1}}{\partial \mathbf{x}_n} \tag{2}$$

where, **F** is the deformation gradient, **f** is the relative deformation gradient, and **I** is the identity unit tensor. In the updated Largrangian formulation, an incremental displacement is defined with respect to the configuration at time $t_n$, which is considered the reference configuration for the current load step. The updated Lagrangian formulation can therefore be visualized as a series of intermediate total Lagrangian formulations. For the reference configuration, the right Cauchy-Green deformation tensor **C** and Green-Lagrange strain tensor **E** are defined as:

$$\mathbf{C} = \mathbf{F}^T\mathbf{F}, \qquad \mathbf{E} = \frac{1}{2}(\mathbf{C} - \mathbf{1}) \tag{3}$$

In the current configuration, a common deformation measure is the left Cauchy-Green deformation tensor **b** is defined as:

$$\mathbf{b} = \mathbf{F}\mathbf{F}^T \tag{4}$$

For finite deformation problem, the stress measure with respect to the reference configuration is named by second Piola-Kirchhoff stress **S**. The Cauchy stress $\boldsymbol{\sigma}$ and the Kirchhoff stress $\boldsymbol{\tau}$ are defined with respect to the current configuration. The relationships among these stresses are as follows:

$$\boldsymbol{\tau} = J\boldsymbol{\sigma} = \mathbf{F}^T\mathbf{S}\mathbf{F} \tag{5}$$

## Hyperelasticity Model for Tire Modeling

Rubber material exhibits a nearly incompressible feature. For rubber material, we postulate the existence of a strain energy density function, **W**, from which stresses can be directly calculated by taking a derivative with respect to a deformation measure. Generally a strain energy density function is expressed in terms of the right Cauchy-Green deformation tensor **C** instead of Green-Lagrange strain tensor **E**. Based on Eq. (5), the Second Piola-Kirchhoff stress tensor **S** can be given by:

$$\mathbf{S} = \frac{\partial W}{\partial \mathbf{E}} = 2\frac{\partial W}{\partial \mathbf{C}} \tag{6}$$

The hyperelasticity strain energy density function **W** is generally expressed in terms of three invariants of **C**, which are:

$$I_C = \mathrm{tr}\mathbf{C}, \quad II_C = \frac{1}{2}\left(I_C^2 - \mathrm{tr}\mathbf{C}^2\right), \quad III_C = \det\mathbf{C} = J^2 \tag{7}$$

Thus, the stress is computed as:

$$\mathbf{S} = 2\frac{\partial W}{\partial I_C}\frac{\partial I_C}{\partial \mathbf{C}} + 2\frac{\partial W}{\partial II_C}\frac{\partial II_C}{\partial \mathbf{C}} + 2\frac{\partial W}{\partial J}\frac{\partial J}{\partial \mathbf{C}} \tag{8}$$

The derivatives of the invariants are derived as follows:

$$\frac{\partial I_C}{\partial \mathbf{C}} = \mathbf{1}, \quad \frac{\partial II_C}{\partial \mathbf{C}} = I_C\mathbf{1} - \mathbf{C}, \quad \frac{\partial J}{\partial \mathbf{C}} = J\mathbf{C}^{-1} \tag{9}$$

As mentioned early, the rubber material is nearly incompressible in deformation and poses a volumetric locking issue. The hyperelasticity strain energy density function is assumed to be composed of two parts [15]:

$$W(I_C, II_C, J) = \underbrace{\overline{W}(I_C, II_C)}_{\text{(deviatoric part)}} + \underbrace{U(J)}_{\text{(volumetric part)}} \tag{10}$$

The deviatoric part and volumetric part are respectively given by:

$$\overline{W}(I_C, J) = \frac{1}{2}\mu\left(J^{-\frac{2}{3}}\mathrm{tr}\mathbf{C} - 3\right), \qquad U(J) = \frac{1}{2}K(J-1)^2 \tag{11}$$

Based on Eq. (8), the deviatoric stress can be calculated as follows:

$$\bar{\mathbf{S}} = 2\frac{\partial \hat{W}}{\partial \mathbf{C}} = \mu\left(J^{-\frac{2}{3}}\mathbf{1} - \frac{2}{3}\mathrm{tr}\mathbf{C}J^{-\frac{5}{3}}\frac{\partial J}{\partial \mathbf{C}}\right) = \mu J^{-\frac{2}{3}}\left(\mathbf{1} - \frac{1}{3}\mathrm{tr}\mathbf{C}\mathbf{C}^{-1}\right) \tag{12}$$

Applying push forward operation to Eq. (12) gives the deviatoric stress in the current configuration as [15].

$$\begin{aligned}\bar{\mathbf{s}} &= \frac{2}{J}\mathbf{F}\frac{\partial \hat{W}}{\partial \mathbf{C}}\mathbf{F}^T = \mu J^{-\frac{5}{3}}\mathbf{F}\left(\mathbf{1} - \frac{1}{3}\mathrm{tr}\mathbf{C}\frac{\partial J}{\partial \mathbf{C}}\right)\mathbf{F}^T \\ &= \mu J^{-\frac{5}{3}}\left(\mathbf{b} - \frac{1}{3}\mathrm{tr}\mathbf{C}\mathbf{1}\right)\end{aligned} \tag{13}$$

The deviatoric modulus in the reference configuration can be give by:

$$\begin{aligned}\bar{\mathbf{D}} &= 4\frac{\partial^2 \hat{W}}{\partial \mathbf{C}\partial \mathbf{C}} = 2\frac{\partial \bar{\mathbf{S}}}{\partial \mathbf{C}} \\ &= \frac{2}{3}\mu J^{-\frac{2}{3}}\left[\frac{1}{3}\mathrm{tr}\mathbf{C}\left(\mathbf{C}^{-1}\otimes\mathbf{C}^{-1}\right) - \mathbf{C}^{-1}\otimes\mathbf{1} - \mathbf{1}\otimes\mathbf{C}^{-1} - \mathrm{tr}\mathbf{C}\frac{\partial \mathbf{C}^{-1}}{\partial \mathbf{C}}\right]\end{aligned} \tag{14}$$

where,

$$\begin{aligned}&\frac{\partial \mathbf{C}^{-1}}{\partial \mathbf{C}} = -\mathbf{C}^{-1}\otimes\mathbf{C}^{-1} \text{ (invariant form)}, \\ &\frac{\partial \mathbf{C}^{-1}_{IJ}}{\partial \mathbf{C}_{KL}} = -\mathbf{C}^{-1}_{IK}\mathbf{C}^{-1}_{JL} \text{ (indicial form)}\end{aligned} \tag{15}$$

The indicial form of Eq. (14) can be expressed as follows:

$$\begin{aligned}\bar{\mathbf{D}}_{IJKL} &= 4\frac{\partial^2 \hat{W}}{\partial \mathbf{C}_{IJ}\partial \mathbf{C}_{KL}} = 2\frac{\partial \bar{\mathbf{S}}_{IJ}}{\partial \mathbf{C}_{KL}} \\ &= \frac{2}{3}\mu J^{-\frac{2}{3}}\left[\frac{1}{3}\mathrm{tr}\mathbf{C}\left(\mathbf{C}^{-1}_{IJ}\mathbf{C}^{-1}_{KL}\right) - \mathbf{C}^{-1}_{KL}\delta_{IJ} - \delta_{KL}\mathbf{C}^{-1}_{IJ} - \mathrm{tr}\mathbf{C}\frac{\partial \mathbf{C}^{-1}_{IJ}}{\partial \mathbf{C}_{KL}}\right]\end{aligned} \tag{16}$$

Performing the push forward operation of Eq. (16) to the current configuration [15, 16], the indicial forms are given as follows:

$$\begin{aligned}\bar{d}_{ijkl} &= \frac{1}{J}F_{iI}F_{jJ}F_{kK}F_{lL}\bar{D}_{IJKL} \\ &= \frac{2}{3}\mu J^{-\frac{5}{3}}\left[\frac{1}{3}\mathrm{tr}\mathbf{C}\delta_{ij}\delta_{kl} - \delta_{kl}b_{ij} - b_{kl}\delta_{ij} - \mathrm{tr}\mathbf{C}\delta_{ik}\delta_{jl}\right]\end{aligned} \tag{17}$$

Based on Eq. (11), the pressure can be defined as follows:

$$p = \frac{dU(J)}{dJ} = K(J-1) \tag{18}$$

The total Cauchy stress is expressed by:

$$\boldsymbol{\sigma} = \bar{\mathbf{s}} + p\mathbf{1} \tag{19}$$

The above material model was implemented as a user subroutine and integrated in commercial finite element code ABAQUS. However, standard implicit finite element formulation cannot effectively handle the dynamic finite sliding contact issue. Dynamic explicit finite element seems to be a good choice to simulate dynamic tire/pavement interaction. In that simulation, tangent modulus is not required.

## Criteria for Pavement Damage

For flexible pavement, pavement damage analysis is performed for both fatigue cracking and permanent deformation. Fatigue cracking is a lot of interconnecting cracks, which is caused by the fatigue failure of asphalt surface or stabilized base under repeated traffic loading. The cracking initiates at the bottom of the asphalt layer or stabilized base where the tensile stress or strain is highest under traffic load. The cracks propagate to the top surface of asphalt layer initially as one or more longitudinal parallel cracks. The progress of fatigue cracking is dependent on the repetition of traffic load. It is generally recognized that the allowable number of traffic load repetitions is related to the tensile strain at the bottom of the asphalt layer. The failure criterion for fatigue cracking is expressed by [1, 17, 18].

$$N_f = f_1\varepsilon_t^{-f_2}E^{-f_3} \tag{21}$$

where, $N_f$ is the allowable number of load repetitions to prevent fatigue cracking; $\varepsilon_t$ is the maximum tensile strain at the bottom of asphalt layer; $E$ is the elastic modulus of asphalt layer; and $f_1$, $f_2$, and $f_3$ are constants determined from laboratory fatigue tests with $f_1$ calibrated to correlate with field performance observations. The Asphalt Institute used 0.0796, 3.291, and 0.854 for the three parameters, respectively. In the Asphalt Institute and Shell design methods [1], the allowable number of load repetitions $N_d$ to limit rutting of permanent deformation is related to the vertical compressive strain $\varepsilon_c$ on top of the subgrade by:

$$N_d = f_4\varepsilon_c^{-f_5} \tag{20}$$

in which $f_4$ and $f_5$ are constants determined from road tests. Values of $f_4$ and $f_5$ used in the paper are $6.15E-07$ and 4.0 [1]. The above two equations will be used to estimate the allowable number of load repetitions to limit pavement damage on fatigue cracking and rutting for flexible pavement.

## Three Dimensional Tire/Pavement Interaction Model and Numerical Study

### Finite Element Model for Tire/Pavement Interaction

The tire model is created purely for research use and does not represent any real tire product. The tire is 981*mm* in diameter and the tread width is 327*mm*. The element size of the tire is around 30 *mm*. A tire consists of tread, sidewall, and shoulder. In the modeling of a tire, three structural components are considered: rim, sidewalls, and tread. The tread and sidewalls are made of rubber and are constructed from fiber-reinforced rubber composites. Generally, the rubber is modeled as incompressible or nearly incompressible hyperelastic material, and the fiber reinforcement is modeled as a linear elastic material. The sidewall is composed of lower, upper, and intermediate carcass. The sidewall is the part of the tire that bridges between tread and bead. The sidewall is reinforced with rubber and fabric plies that provide for strength and flexibility. The sidewall

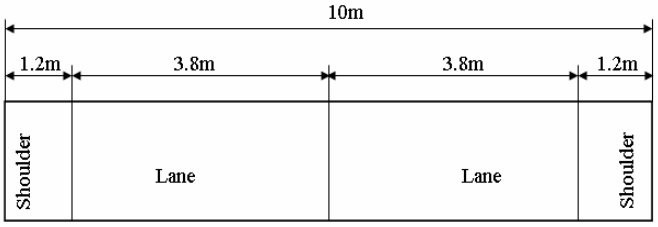


**Fig. 1.** The Geometry of Pavement System.

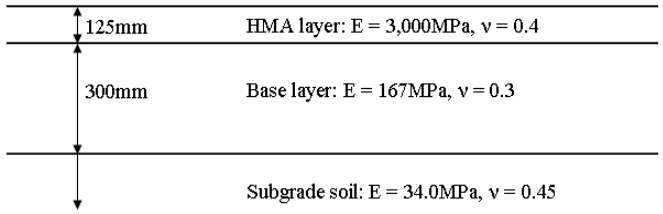


**Fig. 2.** The Material Properties of Pavement System.

transmits the torque applied by the drive axle to the tread in order to create traction. The sidewall, in conjunction with the air inflation, also supports the load of the vehicle. The tread part is the part of tire which comes in contact with the road surface. The tread is made of a thick rubber, or rubber/composite compound formulated to provide an appropriate level of traction that does not wear away too quickly. The tread pattern is characterized by the geometrical shape of the grooves, lugs, and voids, which is not considered detailed in this paper. The entire tire is discretized using an 8-node linear hexahedral element. Therefore, the standard displacement-based finite element model with linear element shows volumetric locking, which underestimates the tire deformation. In order to alleviate the volumetric locking, some mixed and hybrid finite element formulations, such as reduced integration, enhanced/assumed strain, B-bar approach, or mixed displacement-pressure formulation have to be used to model the nearly incompressible hyperelastic material in the nearly incompressible limit. The rim is modeled as a rigid body using kinematic coupling. The kinematic coupling is used to maintain the constant distance between the tire center and bead area. The inflation pressure is applied to the inside surface of tire that can also be modeled using hydrostatic fluid element with ABAQUS/ Explicit and represents fluid-filled cavities under hydrostatic conditions. The vehicle load is applied at each tire hub and acts only in the vertical direction.

The pavement geometry in the transverse direction is shown in Figs. 1 and 2, which is a two-lane and one lane in each traveling direction. The pavement is assumed to deform elastically and the material properties of the three layer system are shown in Fig. 2. For the purpose of simplicity, a symmetric model is selected to model the pavement mechanical behavior under the vehicle load. The analyzed domain of a three-layer pavement is 12,000*mm* in length, 5000*mm* in width, and 3000*mm* in depth. The assumed vehicle has two axles and the load distribution is 60% on rear axle and 40% on front axle. The detailed layout of the four tires can be seen in Fig. 3. Given all the specifications for the tire and pavement structure, Fig. 4 is the three dimensional finite element model for tire/pavement interaction. As shown in Fig. 4, the four-tire vehicle is rolling in the middle of each lane.

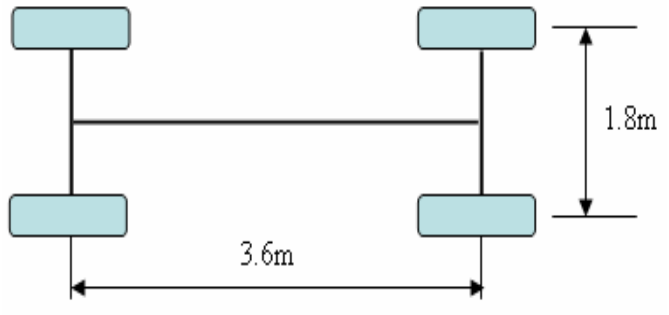


**Fig. 3.** The Layout of a Four-Tire Vehicle.

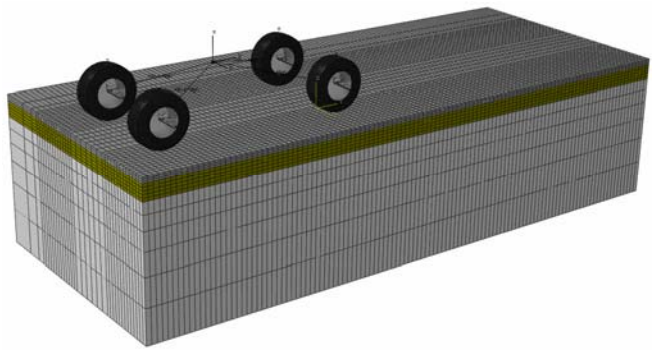

**Fig. 4.** Three Dimensional Finite Element Model of Tire/Pavement Interaction.

All the pavement part is modeled using 8-node hexahedral elements. In order to reduce the number of elements, researchers use fine mesh for the potential tire/pavement interaction area and relatively coarse mesh beyond the contact area. The boundary conditions are fully fixed at the bottom of the domain and only fixed in the normal direction with other surfaces as shown in Fig. 4. Tire/pavement interaction is defined by the contact interface property, which is defined by the tangential friction law. The interaction between tire and asphalt layer is determined by the interfacial frictional contact law. The interfacial behavior related to frictional response is very important to predicting pavement stress state, which controls the transferring of horizontal force and shear stress. Generally the friction between two surfaces can be modeled using the Coulomb model, where a friction coefficient and a shear stress limit are introduced to define the contact interfacial frictional behavior and is obtained from tests. The shear stress transmitted between the two surfaces is computed by multiplying the normal contact stresses across the interface by the coefficient of friction. The drawback of Coulomb frictional law is its inability to capture the rate dependent frictional contact behavior. In this paper, the Coulomb's friction law is temporarily employed to define the tangential friction behavior between tire and terrain. For tire /pavement interaction, pavement is defined as the master surface.

## Tire Footprinting

The aim of this numerical example is to simulate the tire footprint. The numerical test simulates a truck with two axles and four tires. Also, it is assumed that the centroid of vehicle is not exactly in the middle of two axles. The rear axle load is 80*kN* and is applied over

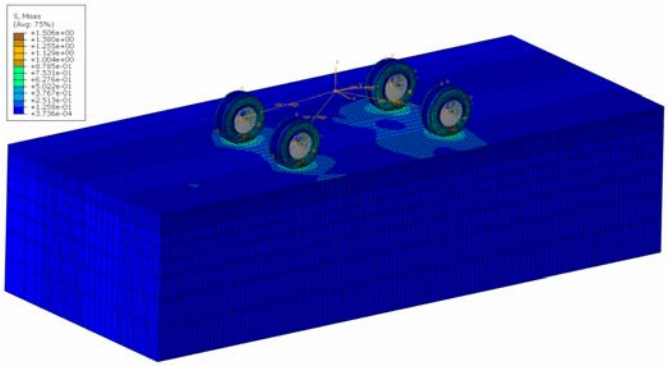

**Fig. 5.** The Stress Contour of Tire/Pavement Interaction.

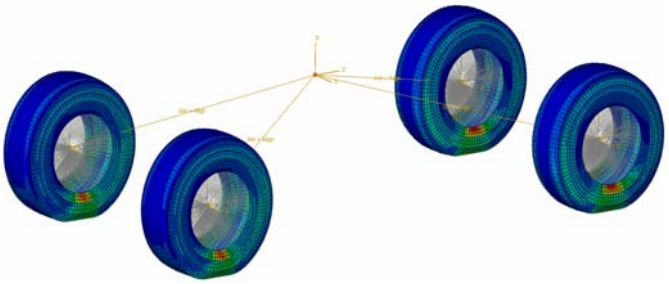

**Fig. 6.** Tire Deformation During Rolling.

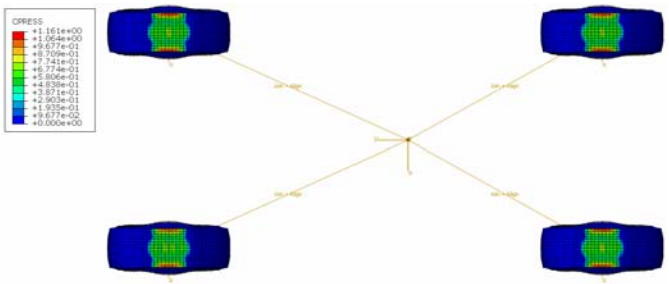

**Fig. 7.** Tire Contact Pressure Under Static Loading.

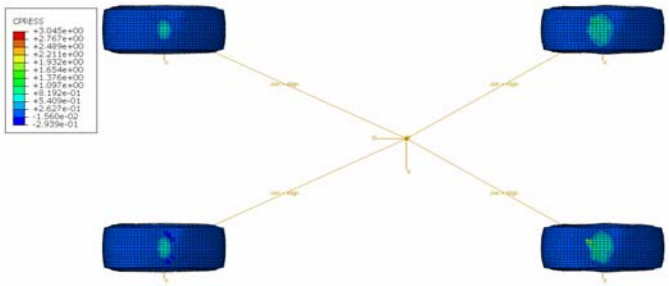

**Fig. 8.** Tire Contact Pressure During Rolling.

two tires. The front axle load is 60*kN*. The tire/pavement interaction model is exactly the same as shown in Fig. 4. The material properties of the pavement part are shown in Fig. 2. The coefficient of friction between tire and pavement is assumed to be 0.5. Fig. 5 shows the Mises stress contour of tire/pavement interaction system at a tire rolling instant. Stress bulbs appear at the tire/pavement contact areas, which indicate stress concentration. Fig. 6 shows the tire footprint on the pavement and the corresponding tire deformation for static and rolling instants. Figs. 7 and 8 show that the contact pressure contour is projected on the deformed tire

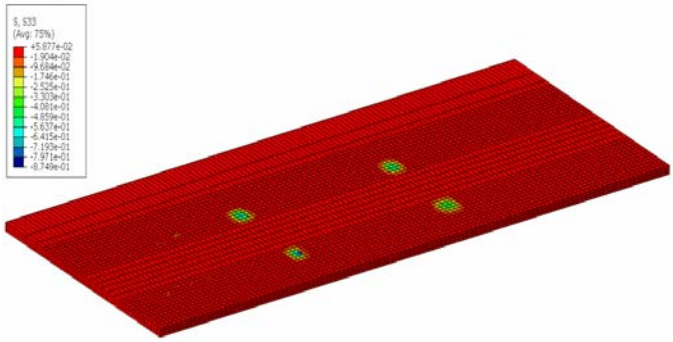

**Fig. 9.** Vertical Stress Contour of the HMA Layer.

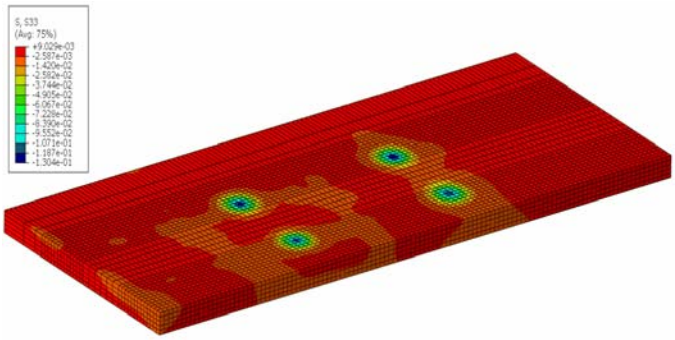

**Fig. 10.** Vertical Stress Contour of the Base Layer.

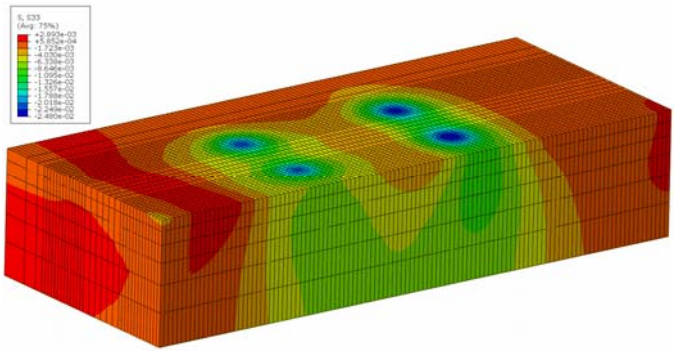

**Fig. 11.** Vertical Stress Contour of Subgrade Soil.

and is not uniformly distributed. Also the shape of tire contact areas is neither rectangle nor circular, which confirms to researchers that the general assumptions made in the previous calculations are not very accurate.

## Application to Predicting Pavement Damage

In this part, researchers obtain the tensile strain at the bottom of asphalt layer and maximum compressible strain at the top of subgrade soil from tire/pavement interaction model to predict fatigue cracking of flexible pavement. The axle load model parameters are exactly same as used for tire footprint. The vehicle is driven through rear axle by applying an angular velocity and is gradually increased to 2*rad/s* within one second. The translation velocity $V_x$ of the tire hub will be gradually increased to the desired value, which is equal to the product of angular velocity and

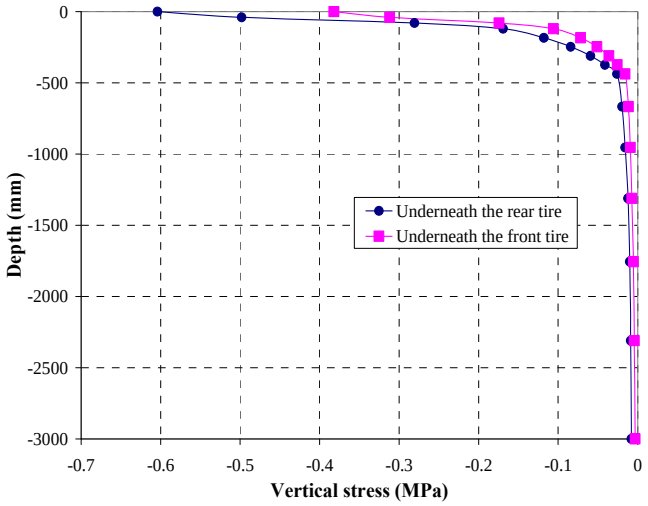


**Fig. 12.** Vertical Stress Versus the Depth of Pavement Structure.

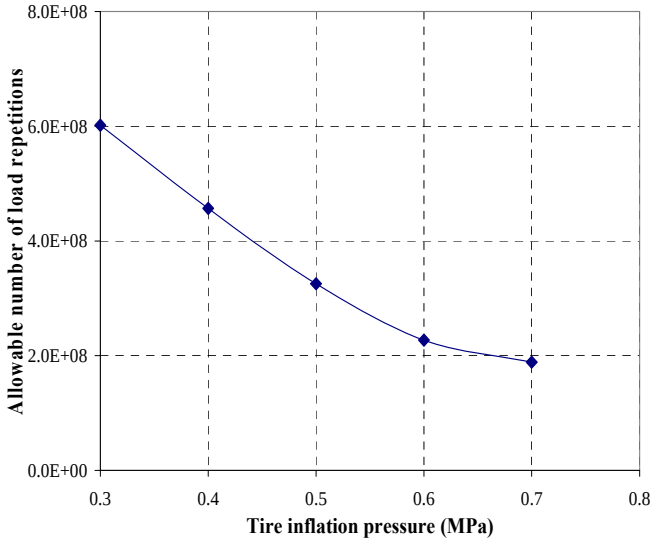


**Fig. 13.** Allowable Number of Load Repetitions to Limit Fatigue Cracking Versus Inflation Pressure.

rolling radius. Figs. 9-11 show the vertical stress (*MPa*) contour projected upon the configurations of asphalt layer, base, and subgrade soil. Clearly, the contact areas are the stress concentrated areas, which have the maximum compressive stress. Fig. 12 shows the vertical stress distribution along the depth of pavement structure, which are extended from the center of tire contact areas. The stress decreases dramatically with depth and agrees very well with field observation or other numerical simulations [1]. Fig. 13 shows the allowable number of load repetitions to limit fatigue cracking, which is obtained based on Eq. (20). The maximum tensile strain at the bottom of asphalt layer is obtained from the three dimensional finite element models. Fig. 14 shows the allowable number of load repetitions to limit rutting or permanent deformation, which is obtained based on Eq. (21). The compressive strain at the top of subgrade soil is also obtained from the three dimensional finite element model. Based on the prediction, the rutting is the dominant concern for this

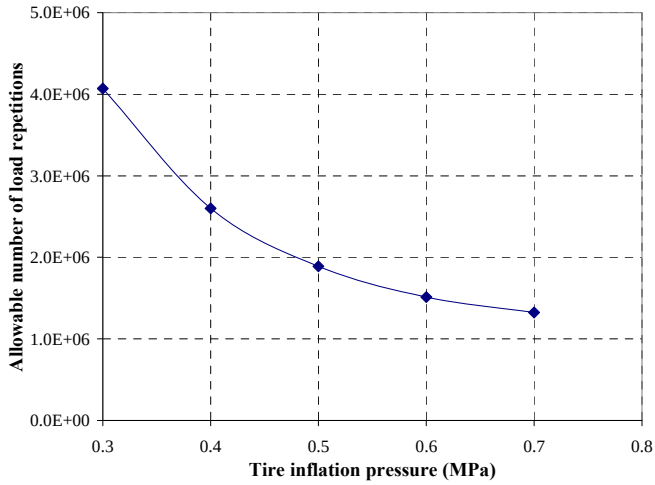


**Fig. 14.** Allowable Number of Load Repetitions to Limit Permanent Deformation Versus Inflation Pressure.

pavement system. Both allowable numbers of load repetitions to limiting fatigue cracking and rutting decrease when the tire inflation pressure is increased. The reason is that the tire becomes stiffer with increasing inflation pressure. Under the same axle load and given tire structure, the tire contact area will decrease and therefore increase contact pressure. Relatively higher tensile strain and compressive strain for both asphalt layer and subgrade soil are produced for a higher inflation pressure compared to lower inflation pressure. Lower inflation pressure will increase contact area and accordingly reduce the strain and stress within pavement structure and, therefore, extend the pavement service life. But low inflation pressure vehicle consumes much more energy than high inflation pressure vehicle.

## Concluding Remarks

In this paper, a finite strain hyperelasticity model for rubber material and three dimensional finite element models for tire/pavement interaction are developed. For tire rolling over flexible pavement, two negative impacts of vehicle on pavement are fatigue cracking and rutting, which have been studied empirically in the past. The criteria for fatigue cracking and rutting need the input of tensile strain at the bottom of the asphalt layer and maximum compressive strain on the top of subgrade soil, which are used to estimate the allowable number of load repetitions to limit fatigue damage and permanent deformation. The accurate way to calculate these two parameters is to fully conduct tire/pavement interaction analysis. This has rarely been done in the past. In order to accurately model tire/pavement interaction, a tire has to be modeled as deformable body and better modeled as finite strain hyperelasticity, which was done in this paper and rarely conducted in previous research. Some technical issues on developing finite element models for tire/pavement interaction were discussed in this paper. A lot of efforts need to be further pursued on the tire/pavement interaction topic to better understanding pavement damage. This paper simply offers a full picture on modeling tire/pavement interaction, which is an issue of great significance on the application of finite element techniques to pavement engineering.

## References


1. Huang, Y.H., (1993). *Pavement Analysis and Design*, Prentice Hall, NJ, USA.
2. Sebaaly, P.E., (1992). Pavement Damage as Related to Tires, Pressures, Axle Loads, and Configurations. *Proceeding of Vehicle, Tire, Pavement Interface*, ISBN: 0-8031-1483-4, Vol.44, pp. 54-68, USA.
3. Sebaaly, P.E. and Tabatabace, N., (1993). Influence of Vehicle Speed on Dynamic Loads and Pavement Response, *Transportation Research Record*, No. 1410, pp. 107-114.
4. Dai, S.T., Deusen, D., De Beer, M., Rettuer, D., and Cochran, G., (1997). Investigation of Flexible Pavement Response to Truck Speed and FWD Load Through Instrumented pavements, , *Proceeding of the 8th International Conference on Asphalt Pavements*, Vol. 1, pp. 141-158, Seattle, WA, USA.
5. Pascale, P., Dore, G., and Prophete, F., (2004). Characterization of Tire Impact on the Pavement Behavior, *Canadian Journal of Civil Engineering*, 31(5), pp. 860-869.
6. Siddharthan, R., Krishnamenon, N., El-Mously, M., and Sebaaly, P.E., (2000). Investigation of Tire Contact Stress Distribution on Pavement Response, *Journal of Transportation Engineering*, 128(2), pp. 136-144.
7. Al-Qadi, I.L., Yoo Pyeong, J., Elseifi, M.A., and Janajreh, I., (2005). Effects of Tire Configurations on Pavement Damage, *Journal of the Association of Asphalt Paving Technologists*, Vol. 74, pp. 921-961.
8. Al-Qadi, I.L., Loulizi, A., Janajreh, I., and Freeman, T.E., (2002). Pavement Response to Dual and New Wide-Base Tires at the Same Tire Pressure, *Transportation Research Record,* No. 1806, pp. 38-47.
9. De Beer, M., Fisher, C., and Jooste, F.J., (1997). Determination of Pneumatic Tire/Pavement Interface Contact Stresses under Moving Loads and Some Effects on Pavements with Thin Asphalt Surfacing Layers, *Proceeding of the 8th International Conference on Asphalt Pavements*, pp.179-227, University of Washington, Seattle, WA, USA.
10. Hua J. and White, T., (2002). A Study of Nonlinear Tire Contact Pressure Effects on HMA Rutting, *International Journal of Geomechanics*, 2(3), pp. 353-376.
11. Park, D., Martin, A.E., and Masad, E., (2005). Effects of Nonuniform Tire Contact Stresses on Pavement Response, *Journal of Transportation Engineering,* 131(11), pp. 873-879.
12. Yoo, P.J., Al-Qadi, I.L., Elseifi, M.A., and Nanajreh, I., (2006). Flexible Pavement Responses to Different Loading Amplitudes Considering Layer Interface Condition and Lateral Shear Forces, *International Journal of Pavement Engineering*, 7(1), pp.73-86.
13. Kim, D., Salgado, R., and Altschaeffl, A.G., (2005). Effects of Supersingle Tire Loadings on Pavements, *Journal of Transportation Engineering*, 131(10), pp. 732-743.
14. Ong, G.P. and Fwa, T.F., (2007). Wet-Pavement Hydroplaning Risk and Skid Resistance: Modeling, *Journal of Transportation Engineering*, 133(10), pp. 590-598.
15. Sun, L., Hudson, W.R., and Zhang, Z., (2003). Empirical-Mechanistic Method Based Stochastic Modeling of Fatigue Damage to Predict Flexible Pavement Cracking for Transportation Infrastructure Management, *Journal of Transportation Engineering*, 29(2), pp. 109-117.
16. Sun, L. and Hudson, W.R., (1993). Probabilistic Approaches for Pavement Fatigue Cracking Prediction Based on Cumulative Damage Using Miner's Law, *Journal of Engineering Mechanics*, Vol. 131, pp. 546-549.
17. Simo, J.C. and Hughes, T.J.R., (1993). *Computational Inelasticity*, Springer-Verlag, USA.
18. Belytschko, T., Liu, W.K., and Moran, B., (2000). *Nonlinear Finite Elements for Continua and Structures*. John Wiley & Sons Ltd, UK.